<Original Paper>

Journal of the Korean Society for Nondestructive Testing, Vol. 36, No. 1: 1-8, 2016
ISSN 1225-7842 / eISSN 2287-402X *http://dx.doi.org/10.7779/JKSNT.2016.36.1.1*

Comparison of Slowness Profiles of Lamb Wave with Elastic Moduli and Crystal Structure in Single Crystalline Silicon Wafers

Youngjae Min*,**, Gyeongwon Yun*,**, Kyung-Min Kim*,***, Yuji Roh*,** and Young H. Kim*†

Abstract Single crystalline silicon wafers having (100), (110), and (111) directions are employed as specimens for obtaining slowness profiles. Leaky Lamb waves (LLW) from immersed wafers were detected by varying the incident angles of the specimens and rotating the specimens. From an analysis of LLW signals for different propagation directions and phase velocities of each specimen, slowness profiles were obtained, which showed a unique symmetry with different symmetric axes. Slowness profiles were compared with elastic moduli of each wafer. They showed the same symmetries as crystal structures. In addition, slowness profiles showed expected patterns and values that can be inferred from elastic moduli. This implies that slowness profiles can be used to examine crystal structures of anisotropic solids.

Keywords: Silicon Single Crystal, Crystal Structure, Slowness, Lamb Wave, Elastic Constants

1. Introduction

Lamb wave (LW) is generated when an acoustic wave propagates inside solid plates. Waves reflected and incident to the boundary surface combine to form different modes of the plate waves. LW is one of these plate waves. When mode conversion of shear vertical waves and longitudinal waves occurs and both waves combine at the boundary of the plate, LW is formed.

Unlike bulk waves, LW has dispersive property, which causes the phase velocities to be dependent on the product of the frequency and the thickness of the (isotropic) plate. Infinitely many modes exist all over the frequency. LW can be detected using immersion ultrasonic testing [1]. When an acoustic wave of certain frequency is directed toward plates immersed in water, phase matching takes place at a certain incident angle, and LW is generated. While propagating along the plate, energy leakage occurs.

Adopting previous research results on back reflection of ultrasound obliquely incident to solid surface in water was observed [2], one can acquire pulse-echo responses from the liquid/ solid boundary due to a phenomenon called the ultrasonic backward radiation of propagating Rayleigh surface wave [3]. Backward radiations were classified into backscattering, leaks of microstructural scattering, and edge reflected radiations [4]. Backscattered LLWs have been measured for isotropic plates [5], and for anisotropic fibrous composite laminates [6].

When a LW propagates inside an anisotropic plate, phase velocity is not only affected by the thickness of the plate and the frequency of the propagating LW, but also by the propagation direction. Material anisotropy has a strong influence on the velocities, attenuation, and acoustic energy of the LW [7]. Rayleigh angle of backward radiation was measured in a single crystalline nickel [8], and phase velocities were determined at each of the various incident

[Received: October 28, 2015, Revised: January 10, 2016, Accepted: January 25, 2016] *Applied Acoustics Lab, Korea Science Academy of KAIST, Busan 47162, Korea, **Korea Advanced Institute of Science and Technology, Daejeon, 34141, Korea, ***Seoul National University, Seoul 08826, Korea †Corresponding Author: yhkim627@kaist.ac.kr
ⓒ 2016 Korean Society for Nondestructive Testing

angles. Velocity distribution was recorded on the plate as dots, and crystalline structure and defects were evaluated. In addition, Park and Kim examined anisotropy of LW in a single crystalline silicon wafer and compared the result with that in isotropic aluminum [9].

Silicon is one of the well-known materials, and simple cubic interpretation of silicon crystal structure enabled immense theoretical analysis of silicon wafers [10]. A proper coordinate transformation to the known stiffness tensor gives the elastic constants for a given propagation direction.

In the present work, immersion ultrasonic testing was used as a method to investigate slowness profiles of LW in (100), (110), and (111) direction of silicon wafers. The slowness profiles were compared with elastic moduli and crystal structures.

2. Theoretical Background

2.1. Leaky Lamb Wave

Fig. 1 shows schematic diagram of how LLW is generated and detected. In the present work, edge reflected radiations were employed. When an ultrasound of a single frequency is obliquely incident to the plate, phase matching takes place at specific angles at which the specific modes of LW are generated within the plate, propagated along the plate and reflected at the edge. During the propagation, the energy leaks to the water at the same angle as the incident beam. Some of them can be detected by the same transducer, allowing the pulse-echo setup to detect LLWs reflected at the edge of the specimen. The phase velocity can be calculated by Snell's law with refracted angle being 90° as

$$c_p = \frac{c_w}{\sin\theta_i}, \tag{1}$$

where c_p is the phase velocity of the LW, θ_i is the incident angle of acoustic wave generated

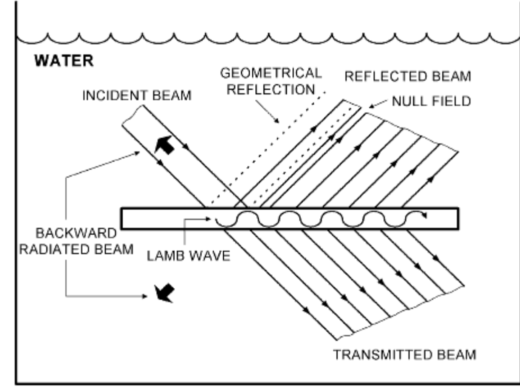

Fig. 1 Schematic diagram for LLW generation

from the transducer, and c_w is the speed of acoustic wave inside water, which is approximately 1500 m/s (or 1.5 mm/μs).

2.2. Elastic Moduli

The silicon single crystal has a diamond structure, however it can be considered as a simple cubic crystal which is consisted of 8 silicon atoms [11]. (100), (110), and (111) shown in Fig. 2 are the most common crystal orientations of silicon crystals [10], and these orientations were considered in the present work. The red spheres in the figures are atoms at corner in unit cell of silicon crystal.

For an isotropic material, Young's modulus is defined as the ratio of stress and strain in the direction of the stretching. That is

$$E = \frac{\sigma_{11}}{\varepsilon_{11}} \tag{2}$$

where stretching direction is x. The Poisson's ratio is defined as ratio of length extension to sideways contraction, that is

$$\mu = \frac{\varepsilon_{22}}{\varepsilon_{11}} \tag{3}$$

For an anisotropic material such as silicon, Young's modulus depends on which crystal direction the material is being stretched to. To account for anisotropy, tensor formalism is required. The general relationship between stress

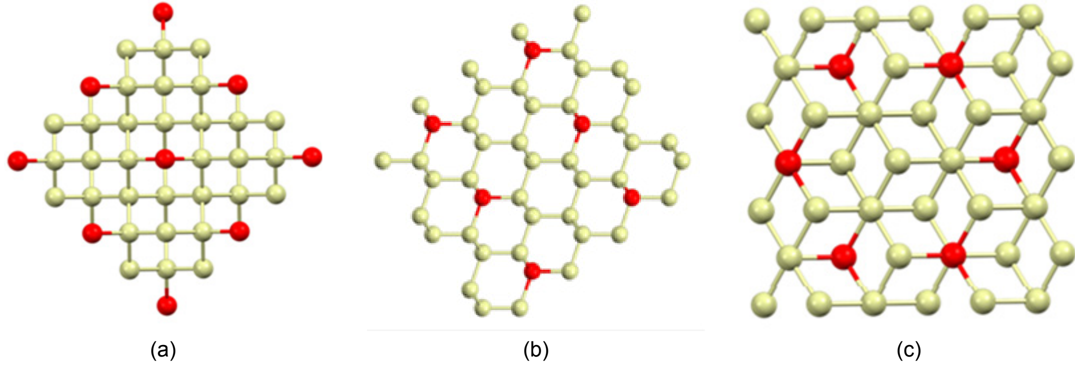

Fig. 2 Crystal structures of (a) (100), (b) (110) and (c) (110) silicon single crystal

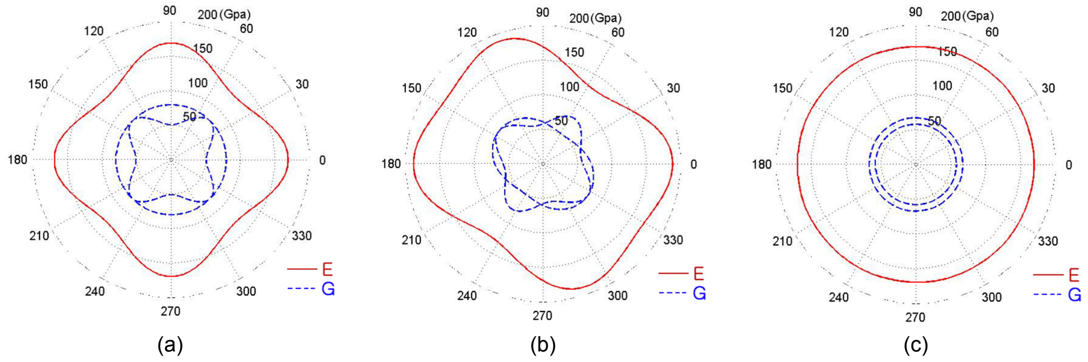

Fig. 3 Elastic moduli of (a) (100), (b) (110) and (c) (111) direction silicon wafers

and strain is [12]

$$\sigma_{ij} = \sum_{k=1}^{3} \sum_{l=1}^{3} c_{ijkl}\, \varepsilon_{kl}, \tag{4}$$

where c_{ijkl} is the stiffness tensor, ε_{kl} is the strain and σ_{ij} is the stress tensor. Stiffness tensor of silicon single crystal in (100) direction is given by

$$c_{ijkl} = \begin{pmatrix} 166 & 64 & 64 & 0 & 0 & 0 \\ 64 & 166 & 64 & 0 & 0 & 0 \\ 64 & 64 & 166 & 0 & 0 & 0 \\ 0 & 0 & 0 & 80 & 0 & 0 \\ 0 & 0 & 0 & 0 & 80 & 0 \\ 0 & 0 & 0 & 0 & 0 & 80 \end{pmatrix} \text{GPa}. \tag{5}$$

Young's modulus in [100] direction can be obtained as [13]

$$E_{[100]} = c_{11} - 2\frac{c_{12}}{c_{11}+c_{12}} c_{12} = 130 \text{ GPa}, \tag{6}$$

and the Poisson's ratio can similarly be obtained as

$$\mu_{[100]} = \frac{c_{12}}{c_{11}+c_{12}} = \quad 0.28 \tag{7}$$

The elastic moduli in any direction can be obtained by calculating the stiffness tensor by rotating coordinates. Rotated stiffness, c^* is obtained by [14]

$$c^*_{ijkl} = \sum_{p=1}^{3} \sum_{q=1}^{3} \sum_{r=1}^{3} \sum_{s=1}^{3} Q_{pi} Q_{qj} Q_{rk} Q_{sl} c_{pqrs}, \tag{8}$$

where Q is the rotation matrix, and is given by

$$Q = \begin{bmatrix} \cos\theta & -\sin\theta & 0 \\ \sin\theta & \cos\theta & 0 \\ 0 & 0 & 1 \end{bmatrix}, \tag{9}$$

when specimen rotates by the angle θ around the z axis.

Young's modulus (E) and shear modulus (G) of a single crystal silicon wafer were calculated by the above methods, and showed in Fig. 3. It is easily found that the elastic moduli of (100) and (110) plates have square and rectangular symmetries, respectively, and (111) plate has isotropic distribution.

3. Experimental Details

3.1. Measurement Setup

(100), (110), and (111) direction silicon wafers were employed. Details of specifications of wafers are as follows:

- Diameter: 100 mm
- Thickness: 525 ± 25 μm
- Type / Dopant: P / B
- Resistivity: 1 ~ 20 ohm·cm
- Surface: one side polished

The effect of doping on elastic behavior is typically a 1~3% decrease for heavy doping levels and usually ignored for engineering calculations [15].

10 MHz single transducer of 15 mm diameter was used to generate and detect the ultrasound in pulse-echo setup. Detailed settings of pulser and receiver are indicated in Table 1.

A fully automated system used for the measurement of edge reflected LLW is shown in Fig. 4. Motor 1 and Motor 2 were employed to change propagation direction and incident angle, respectively. Motor 1 was employed to change the propagation direction from 0º to 360º with 0.5º increment by rotating the specimen while motor 2 was used for controlling the incident angle from 0º to 30º with 0.5º increment by rotating the transducer.

The LW was designated to propagate in the radial direction, so that it is reflected back at the circumference of wafer. The reflected ultra-

Table 1 Setting information of pulser/receiver

Mode	P/E	High pass filter	100 kHz
PRF	1.00 kHz	Low pass filter	20 MHz
Energy	10J	Input attenuation	0.0 dB
Damping	500 ohm	Output attenuation	9.0 dB
		Gain	40 dB

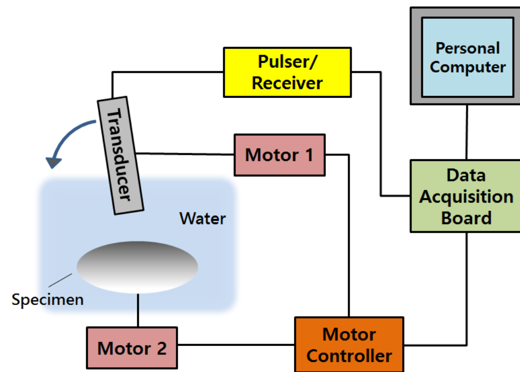

Fig. 4 Experimental apparatus for the measurement of leaky Lamb wave

sound was digitized at 200 MHz sampling rate by 12 bit A/D converter, and stored in personal computer.

3.2. Data Analysis

For each wafer, 61×721 waveforms were stored in personal computer. Fig. 5 shows the procedure to obtain slowness of LW in (111) silicon wafer. Maximum amplitude of signal was extracted for a given incident angle and a propagation direction. As shown in Fig. 5(a), angular profile of edge reflected LLW can be obtained from the maximum amplitude as a function of incident angle [16]. Some waveforms at certain incident angles showed large amplitude compared to other waveforms. It implies that phase matching occurred at those incident angles.

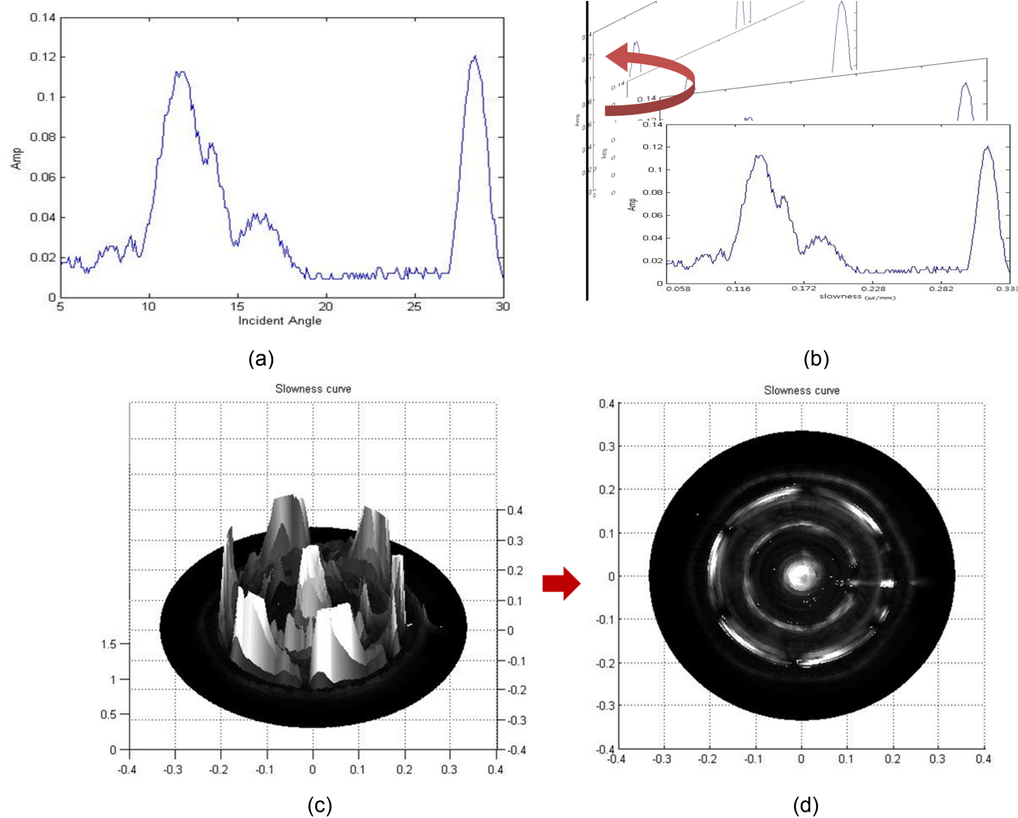

Fig. 5 Procedure to obtain angular profile of LW slowness. (a) angular profile of edge-reflected leaky Lamb wave, (b) slowness profiles for various propagation directions, (c) three dimensional profile of slowness, and (d) slowness profile as a function of propagation direction

Since phase velocity is given by Eq. (1), slowness (inverse of phase velocity) is determined from incident angle. Using this equation, the horizontal axis of Fig. 5(a) is converted into slowness, and this is repeated for various propagation directions. Integrating every graph of each propagation direction makes a three dimensional profile of slowness as shown in Fig. 5(c). By representing height in the three dimensional profile as gray-scaled color, slowness profile shown in Fig. 5(d) is obtained.

4. Results and Discussions

On the polar plane of r and θ, each data was plotted with r representing slowness and θ representing propagation direction. Maximum amplitude was displayed by brightness of points as shown in Fig. 5(d). Applying this process to each data of (100), (110), and (111) direction silicon wafers, final slowness profiles were obtained as shown in Fig. 6. Moreover, phase velocities of LW in a few modes were also obtained by using computer simulation program, *DISPERSE* [17]. With the reciprocals of the calculated velocities, theoretical values were marked on the figures. Different colors and different shapes were used to separate each mode of LW. Unfortunately, the *DISPERSE* program did not work for (111) direction silicon wafer, so it was impossible to compare the slowness profile of (111) direction silicon wafer with theoretical values.

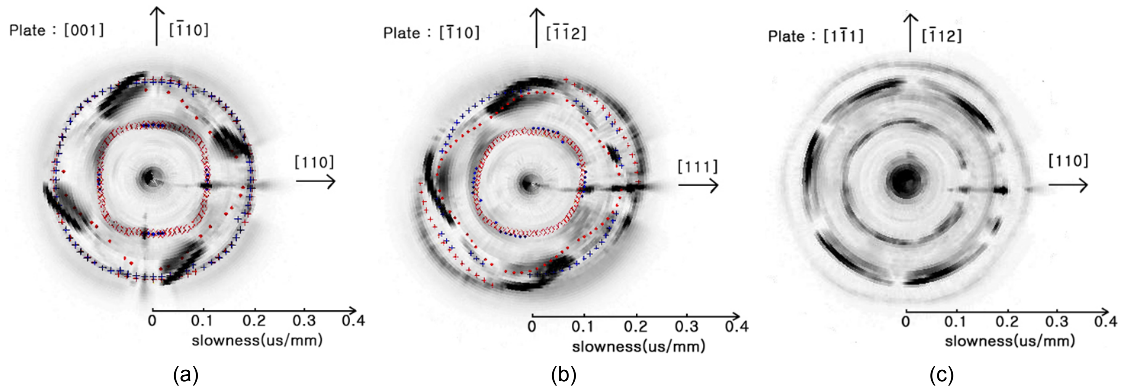

Fig. 6 Slowness profiles of (a) (100), (b) (110) and (c) (110) direction silicon wafers

4.1. (100) Silicon Wafer

The slowness profile of (100) silicon wafer is shown in Fig. 6(a). Three major slowness patterns of LW are observed in slowness profile; from the outermost, circular, diagonal, and round-square shape, respectively. By computer simu- lation, each of them were identified to be the S0, A1, and S1 mode, respectively. These profiles could be also figured out from elastic moduli distribution, which shows diagonal, circular, and rectangular pattern. In slowness profile, symmetric axes are horizontal and vertical lines, which are also found in elastic moduli shown in Fig. 3(a). Furthermore, these symmetries could also be found in crystal structure of (100) silicon wafer as shown in Fig. 2(a).

4.2. (110) Silicon Wafer

Slowness profiles of (110) direction silicon wafer are shown in Fig. 6(b). Total of four major patterns were observed. Two were elliptical and diamond patterns from the outer part. The other two are circular that is right inside the diamond pattern, and the innermost another circular pattern. The symmetric axis is slanted 35° from positive x-axis, which is major axis of elliptical band. The minor axis of elliptical band is also one of the symmetric axis.

In the crystal model of (110) crystal wafer, however, symmetry with the major axis does not match while that of the minor axis does. Interestingly, in the scale of unit cell, the crystal structure is symmetric with the major axis. That symmetry seems like a fault in geometry. The reason for the existence of symmetry of slowness profiles despite the lack of symmetry of crystal structure is that acoustic wave is too big as a probing tool to reveal the symmetry in the atomic scale.

4.3. (111) Silicon Wafer

The slowness profiles of (111) direction silicon wafer are shown in Fig. 6(c). From the outermost part, hexagonal symmetry is repeated and also circular pattern is observable. Elastic moduli shown in Fig. 3(c), however, seem to be an isotropic one. LW propagation is strongly dependent on the elastic moduli, but the slowness profiles of LW showed different pattern from the elastic moduli. On the other hand, hexagonal symmetry of the crystal structure of (111) silicon wafer shown in Fig. 2(c) can be found in the slowness profiles. It implies that slowness profiles of LW are more sensitive to the crystal structure than to the elastic moduli.

4.4. Skew Symmetry

Interestingly, for all specimens, the value of maximum amplitude decreased as the transducer moved counterclockwise of specimen. This implies that the intensity of leaky Lamb wave decreased counterclockwise. This tendency cannot be explained by crystal structure or simple cubic interpretation of it. The symmetry of general pattern can be explained by crystal structure and elastic moduli but skew symmetry is only found in slowness profiles. It may be caused by beam skewing and offset of wave propagation direction from radial direction of specimen.

5. Conclusion

Throughout all the slowness profiles, the patterns of slowness profiles showed symmetries that are expected from the crystal structures of anisotropic plates. The symmetric axes found in the slowness profiles matched with those of crystal symmetries. In (100) and (110) wafers, elastic moduli also had the same symmetries and symmetric axes. Slowness profiles of anisotropic plate reveal symmetry and crystal structure of the plate. In addition, the hexagonal symmetry of slowness profiles of (111) wafer, which is not found in elastic moduli, was also observed. These results can be applied to predict crystal structure of an unknown oriented anisotropic plate through plotting a slowness profile.

Acknowledgment

This work was supported by the Research & Education Program (2012) at the Korea Science Academy of KAIST with funds from the Ministry of Science, ICT and Future Planning.

References

[1] S. J. Song, Y. H. Kim, S. D. Kwon and Y. -M. Cheong, "Determination of phase velocity dispersion curve and group velocity of Lamb waves using backward radiation," *Journal of Acoustical Society of Korea*, Vol. 22, pp. 61-68 (2003)

[2] S. Sasaki, "Back reflection of ultrasonic wave obliquely incident to solid surface in water," *Japanese Journal of Applied Physics*, Vol. 2, pp. 198 (1963)

[3] H. L. Bertoni and T. Tamir, "Unified theory of Rayleigh-angle phenomena for acoustic beams at liquid-solid interfaces," *Applied Physics*, Vol. 2, No. 4, pp. 157-172 (1973)

[4] Y. H. Kim, S.-J. Song, D. H. Bae and S.-D Kwon, "Assessment of material degradation due to corrosion-fatigue using a backscattered Rayleigh surface wave," *Ultrasonics*, Vol. 42, No. 1. pp. 545–550 (2004)

[5] M. de Billy, L. Adler and G. Quentin, "Measurements of backscattered leaky Lamb waves in plates," *Journal of Acoustical Society of America*, Vol. 75, pp. 998-1001 (1984)

[6] D. E. Chimenti and A. H. Nayfeh, "Leaky Lamb waves in fibrous composite laminates," *Journal of Applied Physics*, Vol. 58, pp. 4531-4538 (1985)

[7] M. A. Torres-Arredondo, H. Jung and C. -P. Fritzen, "A study of attenuation and acoustic energy anisotropy of Lamb waves in multilayered anisotropic media for NDT and SHM applications," *6th International Workshop on NDT in Progress*, *Prague, Czech Republic* (2011)

[8] L. Adler, S. -W. Wang, K. Bolland, M. de Billy and G. Q. Jentin, "Rayleigh angle back scattering of ultrasonic beam from single crystal nickel in 111 and 110 planes," *Journal of Acoustical Society of America*, Vol. 77, pp. 1950-1953 (1985)

[9] Y. K. Park and Y. H. Kim, "Lamb waves in an anisotropic plate of a single crystal

silicon wafer," *6th International Workshop on NDT in Progress*, *Prague, Czech Republic* (2011)

[10] J. Kim, D. Cho and R. S. Muller, "Why is (111) silicon a better mechanical material for MEMS?," *Transducers 2001*, Munich, pp. 662-665 (2001)

[11] J. J. Wortman and R. A. Evans, "Young's modulus, shear modulus, and Poisson's ratio in silicon and germanium," *Journal of Applied Physics*, Vol. 36, pp. 153-156 (1965)

[12] H. F. Pollard, "Sound Waves in Solids," Pion Limited, London, pp. 9-15 (1977)

[13] J. F. Nye, "Physical Properties of Crystals: Their Representation by Tensors and Matrices," Oxford University Press, Oxford, pp. 142-145 (1957)

[14] V. Kaajakari, "Silicon as an anisotropic mechanical material - a tutorial," http://www.kaajakari.net/~ville/research/tutorials/tutorials.shtml.

[15] M. A. Hopcroft, W. D. Nix and T. W. Kenny, "What is the Young's modulus of silicon?," *Journal of Microelectromechanical Systems*, Vol. 19, pp. 229-238 (2010)

[16] S. D. Kwon, M. S. Choi and S. H. Lee, "The applications of ultrasonic backward radiation from a layered substrate submerged in liquid," *NDT&E International*, Vol. 33, pp. 275-281 (2000)

[17] B. Pavlakovic and M. J. S. Lowe, "Disperse Version 2.0," Imperial College NDT Lab, London (2002)